

# ***Kif14* overexpression accelerates murine retinoblastoma development**

**Michael O'Hare,<sup>1,2,6</sup> Mehdi Shadmand,<sup>1,2</sup> Rania S. Sulaiman,<sup>1,2,3,7</sup> Kamakshi Sishtla,<sup>1,2</sup> Toshiaki Sakisaka<sup>8</sup> and Timothy W. Corson<sup>1-5</sup>**

<sup>1</sup>Eugene and Marilyn Glick Eye Institute, Departments of <sup>2</sup>Ophthalmology, <sup>3</sup>Pharmacology and Toxicology, <sup>4</sup>Biochemistry and Molecular Biology, and <sup>5</sup>Melvin and Bren Simon Cancer Center, Indiana University School of Medicine, Indianapolis, IN, USA; <sup>6</sup>Biomedical Science, University of Ulster, Coleraine, United Kingdom, <sup>7</sup>Department of Biochemistry, Faculty of Pharmacy, Cairo University, Cairo, Egypt; <sup>8</sup>Division of Membrane Dynamics, Department of Physiology and Cell Biology, Kobe University Graduate School of Medicine, Kobe, Hyogo, Japan

**Short title:** *Kif14* accelerates retinoblastoma formation

**Correspondence to:** Timothy W. Corson, Eugene and Marilyn Glick Eye Institute, 1160 West Michigan Street, Indianapolis, IN 46202 USA, Tel: 1-317-274-3305, Fax: 1-317-274-2277, E-mail: tcorson@iupui.edu

**Keywords:** retinoblastoma, optical coherence tomography, kinesin, oncogene, transgenic mouse.

**Abbreviations:** CIT, citron kinase; H&E, hematoxylin & eosin; IHC, immunohistochemistry; INL, inner nuclear layer; *i.p.*, intraperitoneal; KIF14, kinesin family member 14; OCT, optical coherence tomography; PRC1, protein regulator of cytokinesis 1; TAg, Simian Virus 40 large T antigen; TAg-RB, T antigen-retinoblastoma model; TBS, Tris buffered saline.

**Article category:** Cancer Genetics and Epigenetics, Short report

**Word count:** 2607

**Novelty and impact**

The mitotic kinesin KIF14 is overexpressed and is a prognostic indicator in multiple cancers. This study examined the effect of *Kif14* overexpression on cancer *in vivo* for the first time, using a transgenic murine retinoblastoma model. *Kif14* overexpression accelerated retinoblastoma initiation, growth rate, progression, and total tumor burden in these mice. These findings confirm that *Kif14* can promote tumor progression *in vivo*, further validating KIF14 as an oncogene and potential therapeutic target.

**Abstract**

The mitotic kinesin KIF14 has an essential role in the recruitment of proteins required for the final stages of cytokinesis. Genomic gain and/or overexpression of *KIF14* has been documented in retinoblastoma and a number of other cancers, such as breast, lung and ovarian carcinomas, strongly suggesting its role as an oncogene. Despite evidence of oncogenic properties *in vitro* and in xenografts, Kif14's role in tumor progression has not previously been studied in a transgenic cancer model. Using a novel *Kif14* overexpressing, simian virus 40 large T-antigen retinoblastoma (TAg-RB) double transgenic mouse model, we aimed to determine *Kif14*'s role in promoting retinal tumor formation. Tumor initiation and development in double transgenics and control TAg-RB littermates were documented *in vivo* over a time-course by optical coherence tomography, with subsequent *ex vivo* quantification of tumor burden. *Kif14* overexpression led to an accelerated initiation of tumor formation in the TAg-RB model and a significantly decreased tumor doubling time (1.8 vs. 2.9 weeks). Moreover, overall percentage tumor burden was also increased by *Kif14* overexpression. These data provide the first evidence that *Kif14* can promote tumor formation in susceptible cells *in vivo*.

## Introduction

Retinoblastoma is the most common childhood intraocular malignancy, affecting approximately 1 in 17,000 live births, translating to roughly 8,000 new cases a year globally.<sup>1</sup> Retinoblastoma is the prototypic genetic cancer and has long been a major source of scientific discovery. It is typically initiated by the biallelic loss of the *RBI* gene, which encodes the tumor suppressor, pRB. Although the biallelic loss of *RBI* is (usually) necessary, it is not sufficient to induce retinoblastoma, instead leading to the benign retinoma.<sup>2</sup> Subsequent mutational events are vital to evolve retinoma to retinoblastoma, including somatic gain of chromosome 1q32.<sup>2,3</sup> The minimal region of gain at 1q32 contains *KIF14*, which represents a candidate oncogene in the development of retinoblastoma.<sup>4</sup> The *KIF14* locus is gained in >50% of retinoblastomas,<sup>5</sup> and this gene is over-expressed in 90% of retinoblastomas.<sup>4,6</sup>

KIF14 is a member of the kinesin superfamily;<sup>7</sup> kinesins are molecular motors involved in intracellular transport. KIF14 is essential for cytokinesis, interacting with and helping to localize protein regulator of cytokinesis 1 (PRC1) and citron kinase (CIT).<sup>8</sup> However KIF14 also has cytokinesis independent roles, including negative regulation of Rap1a-Radil signaling at the cell membrane.<sup>9</sup> Although the exact molecular functions of KIF14 are still under investigation, a large body of evidence implicates it as an oncogene.<sup>10</sup> It is gained at the DNA level in tumors such as hepatocellular, renal, and ovarian carcinoma.<sup>10</sup> It is overexpressed in multiple cancer types such as breast (including in premalignant breast tissue of *BRCAl/2* mutation carriers),<sup>11</sup> lung, ovarian, hepatocellular, and brain tumors. Moreover, in these cancers KIF14 levels are prognostic for outcome. KIF14 knockdown decreases tumorigenicity *in vitro* and in xenografts, while overexpression enhances growth.<sup>10</sup>

Despite these exciting findings, the effects of *Kifl4* overexpression in a transgenic cancer model have not previously been assessed. The recent development of a *Kifl4* overexpressing transgenic mouse, constitutively expressing *Kifl4* under a cytomegalovirus promoter,<sup>12</sup> makes such studies possible. Given the importance of KIF14 in human retinoblastoma, we sought to assess the effects of *Kifl4* overexpression on tumor formation in the widely used simian virus 40 T-antigen expressing mouse model of retinoblastoma (TAg-RB).<sup>13</sup>

## Methods

### *Animals*

All animal experiments were approved by the Indiana University School of Medicine Institutional Animal Care and Use Committee (Protocol 10521) and adhered to all standards set forth in the ARVO Statement for the Use of Animals in Ophthalmic and Visual Research. By crossing transgenic mice constitutively overexpressing *Kif14* (BDF1-Tg(pCAGGS-Kif14)#28; Accession Number CDB0476T, <http://www.cdb.riken.jp/arg/TG%20mutant%20mice%20list.html>)<sup>12</sup> into the TAg-RB strain (CB6-Tg(TagRb)1Plm/Mmjax)<sup>13, 14</sup> we generated novel *Kif14*;TAg-RB double transgenic mice. In order to ensure near-congenicity and minimize animal to animal variability in phenotype, the *Kif14* mice (generated in a BDF-1 background) were first backcrossed into the C57BL/6 background for 6 generations. Hemizygous 6th generation *Kif14* backcross offspring were bred with hemizygous TAg-RB mice to obtain double transgenic mice of mixed sex as well as single transgenic TAg-RB or *Kif14* littermates. Mice were genotyped as described.<sup>12, 14</sup> The mice of the desired genotypes were maintained for up to 12 weeks under standard housing conditions.<sup>14</sup>

### *Imaging*

Animal eyes were imaged longitudinally from two weeks (when eyes first opened) to 12 weeks of age. Image-guided optical coherence tomography (OCT) and brightfield funduscopy were performed using a Micron III intraocular imaging system (Phoenix Research Labs; Pleasanton, CA). Animals were sedated with a mix of *i.p.* ketamine (17.2 mg/kg) and dexmedetomidine (0.5 mg/kg). Post sedation, the pupils were dilated using 1% tropicamide, followed by application of a topical hypromellose ophthalmic demulcent solution (Gonak; Akorn, Lake Forest, IL), which prevented the drying of the cornea and the formation of cataracts. After imaging the sedation was reversed by *i.p.* atipamezole (1 mg/kg).

### *Quantification of OCT Images*

In order to quantify the volumes of individual tumors via OCT, we adapted a previously developed ellipsoid volumetric calculation method.<sup>15</sup> The widest sections of the tumors from perpendicular planes were used to calculate ellipsoid volume ( $V$ )

using the formula  $V = 4/3\pi abc$  where  $a$ ,  $b$ , and  $c$  are the radii of the three axes of the ellipsoid.<sup>15</sup> ImageJ 1.49 (<http://imagej.nih.gov>) was used to measure the radii of each tumour from OCT images.

### ***Eye Preparation and Immunohistochemistry***

After intraocular imaging, cohorts of mice were euthanized at 8 and 12 weeks of age. Enucleated eyes were fixed in 4% paraformaldehyde overnight and then transferred to 70% ethanol. The eyes were processed at the Indiana University School of Medicine Histology Core. Whole eyes were embedded in paraffin, then 2–3 papillary-optic nerve 5  $\mu\text{m}$  sections were collected every 300  $\mu\text{m}$  through each globe. Mayer's hematoxylin and eosin (H&E) staining was performed as previously described,<sup>14</sup> while adjacent sections were left unstained for immunohistochemistry (IHC). These sections were deparaffinized with xylenes and an ethanol series, boiled in citrate buffer for 5 minutes, blocked for one hour with 1% normal goat serum in Tris buffered saline (TBS), then probed overnight at 4°C with a TAg antibody (sc-147, Santa Cruz Biotechnology, Santa Cruz, CA) diluted 1:200 in TBS. Detection was performed using the ABC Staining Kit (Santa Cruz Biotechnology) according to the manufacturer's instructions.

### ***Quantification of Immunohistochemistry***

Bright-field micrographs were taken with an EVOS-fl digital microscope (AMG, Mill Creek, WA). Adjacent images of the retina on each slide were stitched together using Adobe Photoshop CS4. ImageJ was used to calculate the percent tumor burden as described.<sup>16</sup> Briefly, the image was converted to 8-bit, then the retinal area was traced manually by an investigator masked to genotype, with area recorded by the region of interest function. Subsequently, the auto threshold function was used to select the TAg expressing cells based on IHC staining. Then, the stained pixels within the retina were counted using the measure function to obtain a value for tumor area in pixels. Total tumor area across the 6–7 slides per globe was divided by total retinal area to obtain the percent tumor area. To provide further validation of this approach, tumor areas histopathologically evident by H&E staining were assessed in a similar manner.

### **qPCR**

RNA was extracted from H&E stained sections (20–24 sections/eye). After coverslip removal in xylene, tissue was scraped into ethanol and RNA extracted using a RecoverAll Total Nucleic Acid Kit (Thermo Fisher, Carlsbad, CA, USA), following the manufacturer's instructions. DNA was removed with a TURBO DNA-free kit (Thermo Fisher), then 90 ng RNA was reverse transcribed with iScript Select (Bio-Rad, Hercules, CA, USA). qPCR was performed on a ViiA7 thermal cycler, using Fast Advanced Master Mix and TaqMan assays for *Kif14* (Mm01291408\_m1), normalized to *Hprt* (Mm01545399\_m1) and *Tbp* (Mm00446973\_m1) (Thermo Fisher). Control reactions lacking reverse transcriptase confirmed removal of genomic *Kif14* transgene sequence.

### **Statistical Analysis**

The independent Student's *t*-test was used to test for differences in tumor number and percent tumor burden between the control eyes and double transgenic eyes harvested at each time point. The extra sum of squares *F*-test was used to assess if the fitted exponential growth curve was shared between genotypes. All analyses were performed with GraphPad Prism v. 6.0, and differences were considered statistically significant at  $p < 0.05$ .

### **Results**

To determine the effect of *Kif14* overexpression on tumor growth in a genetic cancer model, we monitored retinoblastoma progression longitudinally in *Kif14*;TAg-RB double transgenic mice and their single transgenic TAg-RB littermates using OCT. Single TAg-expressing, tumor initiating cells are first observed in the inner nuclear layer (INL) of the retinas of TAg-RB mice at postnatal day 8, and go on to form scattered pre-tumorous cell clusters by 4 weeks of age, before apoptosis kills off most cells, allowing surviving cells to form frank tumors.<sup>17</sup> However, compared to this previously documented growth pattern seen in the TAg-RB mice, the *Kif14*;TAg-RB double transgenics exhibited a dramatically accelerated formation of tumor-like clusters of hyper-reflective cells in the INL from as early as two weeks of age. In the double transgenic mice, these clusters filled the INL by three to four weeks of age, while small clusters remained scattered in the single transgenic mice (Figure 1). At these early ages, no pathology was evident in the fundus photographs of any mouse. Moreover, no abnormalities were seen in the eyes of *Kif14* single transgenic mice

(Figure 1j). We confirmed that *Kif14* mRNA was overexpressed in TAg-RB eyes (on average 5-fold over normal at 12 weeks), and further increased in *Kif14*;TAg-RB eyes (20-fold over normal).

Consistent with increased tumor initiation, *Kif14* overexpression in TAg-RB also promoted an increased tumor number per eye and increased growth rate in the double transgenic mice compared to the single transgenic littermates (Figure 2). OCT and corresponding fundus images from weeks 8 and 12 showed tumors in the INL. The *Kif14*;TAg-RB mice had large groups of tumors visualized as pale masses in the fundus images and hyper-reflective intraretinal masses by OCT compared to relatively isolated tumors in the TAg-RB mice. Indeed, counting of individual tumors in these images suggested a trend towards increased number of tumors per eye in the double transgenics at both week 8 and week 12 (Figure 2e).

A limitation of OCT analysis of TAg-RB eyes is that the extreme periphery of the retina cannot be imaged effectively without distortion, therefore total tumor volume calculations per eye cannot be reliably performed *in vivo* and some tumors may not have been countable by this method. However, in order to monitor tumor growth rate over a time course, volumetric analysis using an ellipsoid volumetric estimation<sup>15</sup> of individual, centrally located tumors from eyes of *Kif14*;TAg-RB and TAg-RB mice over a six week time course was performed. Despite some variability between tumors, this analysis revealed a significant decrease in doubling time of individual tumors in the double vs. single transgenics, 1.8 weeks vs. 2.9 weeks respectively ( $p < 0.0001$ ) (Figure 2f).

We also assessed total tumor burden per eye by *ex vivo* quantification, using expression of TAg as an immunohistochemical marker<sup>16</sup> (which specifically stains viable tumor cells in this model) or by histopathology (which also includes necrotic tumor cores). The overexpression of *Kif14* in TAg-RB resulted in an increased total tumor burden (Figure 3), irrespective of quantification method. At week 8 there was approximately two-fold more tumor burden per eye in the double vs. single transgenic mice ( $p < 0.05$ ) and this increase was even more marked at week 12 ( $p < 0.01$ ).

## Discussion

We show that the overexpression of *Kif14* accelerates tumor onset and increases tumor burden and tumor proliferation rate in the TAg-RB retinoblastoma model. This provides strong evidence that KIF14 is indeed an oncogene, when considered in concert with previous clinical, *in vitro* and xenograft findings.<sup>10</sup>

Over-expression of *Kif14* in TAg-RB led to an acceleration of tumor formation visualized by OCT from as early as week 2. This suggests that Kif14 plays a role in enabling tumor initiation, at least in the context of TAg overexpression. The potent oncoprotein TAg blocks the function of pRB, p107, p130, and p53, amongst other proteins. This readiness of Kif14 to promote growth once pRB is disabled in the murine retina echoes what is observed genetically in humans, in the transition from benign retinoma (which lacks functional pRB) to proliferating retinoblastoma, which also often harbors genomic gain and overexpression of *KIF14*.

In TAg-RB, the *Kif14*-overexpressing tumor cells likely have increased resistance to apoptosis; a wave of apoptosis normally kills off the majority of TAg-positive cells in TAg-RB eyes around week 4,<sup>17</sup> while many cells remain when *Kif14* is overexpressed. Increased apoptosis is a hallmark of *Kif14* loss in mice<sup>12</sup> or knockdown in cancer cells *in vitro*,<sup>10</sup> so the converse could also be true: *Kif14* overexpression may block apoptosis.

But increased proliferation appears to be at play as well in *Kif14* overexpressing cells. Using a novel adaptation of our ellipsoid volumetric quantification method<sup>15</sup> we found that individual tumors in *Kif14*;TAg-RB mice have significantly faster doubling times than those in their TAg-RB littermates. To our knowledge, this is the first assessment of doubling times for TAg-RB tumors, made possible by *in vivo* imaging. Interestingly, the observed doubling times in the *Kif14*;TAg-RB mice are quite comparable to those that have been reported for human retinoblastomas (on the order of 15 days).<sup>18</sup> Increased proliferation of *Kif14* overexpressing tumor cells is consistent with previous *in vitro* work. Overexpression of *KIF14* in hepatocellular carcinoma, lung and ovarian cancer cell lines markedly increased their proliferation capacity,<sup>10</sup> and a similar effect was seen in immortalized mammary epithelial cells.<sup>11</sup> It will be interesting to assess if *Kif14* loss in the context of TAg-RB would slow tumor growth, as it does in cell and xenograft models. Since *Kif14* knockout is lethal by 21 days of

age in mice<sup>12</sup> and embryonic lethal in humans,<sup>19</sup> development of conditional knockouts of *Kif14* to cross into TAg-RB would be required to address this question. Alternatively, since *Kif14* is a druggable ATPase enzyme,<sup>20</sup> novel small molecule treatments<sup>11</sup> could be trialed in TAg-RB mice.

The TAg-RB mouse provides a useful model to test genetic manipulations in retinoblastoma. It was previously used to demonstrate the *in vivo* tumor suppressive roles of *Cdh11*<sup>21</sup> and p75<sup>NTR</sup>.<sup>22</sup> But it has not previously been shown that a putative oncogene can *accelerate* tumor growth in the TAg-RB model, as we have done here. TAg-RB has a number of advantages over other retinoblastoma mouse models, as it bears strong resemblance to the human tumors. It shares the expression pattern of a number of genes, including *Kif14*, with the human disease,<sup>17</sup> and it is the most commonly used model of retinoblastoma for preclinical studies.<sup>23</sup> The tumors initiate in the INL, a possible layer of origin of human tumors, and they contain both Flexner-Wintersteiner and Homer Wright rosettes, histopathological hallmarks of human retinoblastoma that are not seen together in other mouse models of retinoblastoma.<sup>13</sup>

However, the TAg-RB model has limitations. Induced by specific expression of TAg rather than genetic loss of *Rb1*, it has a different molecular etiology from the human disease. Recent work has shown that human retinoblastoma can arise from a cone precursor,<sup>24</sup> while the TAg-RB cell of origin is a Müller glia with progenitor properties;<sup>17</sup> different cell types might respond differently to *Kif14* overexpression. Moreover, since TAg functionally inactivates p53 and other proteins as well as pRB, TAg-RB cells might be particularly susceptible to a putative anti-apoptotic effect of *Kif14* overexpression, whereas the human cell of origin, which may have functional p53, may be less sensitive.

A further limitation of this study is that we used near-congenic rather than completely congenic animals. Thus, we cannot exclude the possibility that a closely linked allele to the *Kif14* transgene could contribute to the observed phenotypic differences. To further support our findings, further backcrosses followed by future investigation of *Kif14* overexpression in other transgenic retinoblastoma models, and in human cell xenograft models of the disease is warranted.<sup>25</sup> Future high-resolution analyses of multiple human and murine retinoblastoma genomes, and correlation with

gene expression, will also help to completely define KIF14's importance in retinoblastomagenesis.

In conclusion, we have demonstrated that overexpression of *Kif14* in the TAg-RB model of retinoblastoma enhances tumor formation. We report a sustained and significant increase in percentage tumor burden in double transgenics compared to TAg-RB control mice, providing strong evidence that *Kif14* can promote retinoblastoma growth in susceptible cells *in vivo*. We observed increased tumor growth rates via OCT analysis and furthermore we present a novel approach to document and compare tumor growth in response to genetic manipulations by combining OCT and IHC imaging of this model. Our results further substantiate the role of *Kif14* as an oncogene in the development of retinoblastoma. Given KIF14's importance in other human cancers such as lung, ovarian and breast cancer, it will be exciting to use the *Kif14* overexpression model in combination with other transgenic cancer models to assess the role of *Kif14* in murine epithelial cancers and further validate *Kif14* as a broadly relevant oncogene.

### **Acknowledgements**

We thank Keith Condon, Indiana University School of Medicine Histology Core for his help sectioning the eye samples and carrying out H&E staining, and Helen Dimaras for critical comments on the manuscript. This research was supported by the American Cancer Society IRG-84-002-28, NIH/NCATS KL2TR001106, St. Baldrick's Foundation, and Research to Prevent Blindness, Inc.

## References

1. Dimaras H, Corson TW, Cobrinik D, White A, Zhao J, Munier FL, Abramson DH, Shields CL, Chantada GL, Njuguna F, Gallie BL. Retinoblastoma. *Nat Rev Disease Primers* 2015;1: Article number: 15021.
2. Dimaras H, Khetan V, Halliday W, Orlic M, Prigoda NL, Piovesan B, Marrano P, Corson TW, Eagle RC, Jr., Squire JA, Gallie BL. Loss of *RBI* induces non-proliferative retinoma: increasing genomic instability correlates with progression to retinoblastoma. *Hum Mol Genet* 2008;17: 1363-72.
3. Thériault BL, Dimaras H, Gallie BL, Corson TW. The genomic landscape of retinoblastoma: a review. *Clin Experiment Ophthalmol* 2014;42: 33-52.
4. Corson TW, Huang A, Tsao MS, Gallie BL. *KIF14* is a candidate oncogene in the 1q minimal region of genomic gain in multiple cancers. *Oncogene* 2005;24: 4741-53.
5. Bowles E, Corson TW, Bayani J, Squire JA, Wong N, Lai PB, Gallie BL. Profiling genomic copy number changes in retinoblastoma beyond loss of *RBI*. *Genes Chromosomes Cancer* 2007;46: 118-29.
6. Madhavan J, Coral K, Mallikarjuna K, Corson TW, Amit N, Khetan V, George R, Biswas J, Gallie BL, Kumaramanickavel G. High expression of *KIF14* in retinoblastoma: association with older age at diagnosis. *Invest Ophthalmol Vis Sci* 2007;48: 4901-6.
7. Miki H, Okada Y, Hirokawa N. Analysis of the kinesin superfamily: insights into structure and function. *Trends Cell Biol* 2005;15: 467-76.
8. Gruneberg U, Neef R, Li X, Chan EH, Chalamalasetty RB, Nigg EA, Barr FA. *KIF14* and citron kinase act together to promote efficient cytokinesis. *J Cell Biol* 2006;172: 363-72.
9. Ahmed SM, Thériault BL, Uppalapati M, Chiu CW, Gallie BL, Sidhu SS, Angers S. *KIF14* negatively regulates Rap1a-Radil signaling during breast cancer progression. *J Cell Biol* 2012;199: 951-67.
10. Thériault BL, Corson TW. *KIF14*: a clinically relevant kinesin and potential target for cancer therapy. In: Kozielski F. *Kinesins and Cancer*. Heidelberg: Springer, 2015: 149-70.
11. Singel SM, Cornelius C, Zaganjor E, Batten K, Sarode VR, Buckley DL, Peng Y, John GB, Li HC, Sadeghi N, Wright WE, Lum L, Corson TW, Shay JW. *KIF14* promotes AKT phosphorylation and contributes to chemoresistance in triple-negative breast cancer. *Neoplasia* 2014;16: 247-56, 56 e2.
12. Fujikura K, Setsu T, Tanigaki K, Abe T, Kiyonari H, Terashima T, Sakisaka T. *Kif14* mutation causes severe brain malformation and hypomyelination. *PLoS One* 2013;8: e53490.

13. Windle JJ, Albert DM, O'Brien JM, Marcus DM, Distèche CM, Bernards R, Mellon PL. Retinoblastoma in transgenic mice. *Nature* 1990;**343**: 665-9.
14. Wenzel AA, O'Hare MN, Shadmand M, Corson TW. Optical coherence tomography enables imaging of tumor initiation in the TAg-RB mouse model of retinoblastoma. *Mol Vis* 2015;**21**: 515-22.
15. Sulaiman RS, Quigley J, Qi X, O'Hare MN, Grant MB, Boulton ME, Corson TW. A simple optical coherence tomography quantification method for choroidal neovascularization. *J Ocul Pharmacol Ther* 2015;**31**: 447-454.
16. Dimaras H, Marchong MN, Gallie BL. Quantitative analysis of tumor size in a murine model of retinoblastoma. *Ophthalmic Genet* 2009;**30**: 84-90.
17. Pajovic S, Corson TW, Spencer C, Dimaras H, Orlic-Milacic M, Marchong MN, To KH, Theriault B, Auspitz M, Gallie BL. The TAg-RB murine retinoblastoma cell of origin has immunohistochemical features of differentiated Müller glia with progenitor properties. *Invest Ophthalmol Vis Sci* 2011;**52**: 7618-24.
18. Abramson DH, Scheffler AC, Beaverson KL, Rollins IS, Ruddat MS, Kelly CJ. Rapid growth of retinoblastoma in a premature twin. *Arch Ophthalmol* 2002;**120**: 1232-3.
19. Filges I, Nosova E, Bruder E, Tercanli S, Townsend K, Gibson WT, Rothlisberger B, Heinemann K, Hall JG, Gregory-Evans CY, Wasserman WW, Miny P, Friedman JM. Exome sequencing identifies mutations in *KIF14* as a novel cause of an autosomal recessive lethal fetal ciliopathy phenotype. *Clin Genet* 2014;**86**: 220-8.
20. Basavarajappa HD, Corson TW. KIF14 as an oncogene in retinoblastoma: a target for novel therapeutics? *Future Med Chem* 2012;**4**: 2149-52.
21. Marchong MN, Yurkowski C, Ma C, Spencer C, Pajovic S, Gallie BL. *Cdh11* acts as a tumor suppressor in a murine retinoblastoma model by facilitating tumor cell death. *PLoS genetics* 2010;**6**: e1000923.
22. Dimaras H, Gallie BL. The p75<sup>NTR</sup> neurotrophin receptor is a tumor suppressor in human and murine retinoblastoma development. *Int J Cancer* 2008;**122**: 2023-9.
23. Nair RM, Vemuganti GK. Transgenic models in retinoblastoma research. *Ocul Oncol Pathol* 2015;**1**: 207-13.
24. Xu XL, Singh HP, Wang L, Qi DL, Poulos BK, Abramson DH, Jhanwar SC, Cobrinik D. Rb suppresses human cone-precursor-derived retinoblastoma tumours. *Nature* 2014;**514**: 385-8.
25. Corson TW, Samuels BC, Wenzel AA, Geary AJ, Riley AA, McCarthy BP, Hanenberg H, Bailey BJ, Rogers PI, Pollok KE, Rajashekhar G, Territo PR. Multimodality imaging methods for assessing retinoblastoma orthotopic xenograft growth and development. *PLoS One* 2014;**9**: e99036.

## Figure Legends

**Figure 1.** *Kifl4* overexpression accelerates tumor initiation in TAg-RB. Increased tumor burden in *Kifl4*;TAg-RB mice (*b, c, e, f, h, i*) vs. TAg-RB controls (*a, d, g*); the retinas of *Kifl4* single transgenic mice were normal (*j*). Representative images at 2–4 weeks of age as visualized by fundus images (upper panels) and OCT (lower panels). Example tumor cell clusters are marked (yellow arrowheads); the entire inner nuclear layer was filled with early tumor cells in some double transgenic eyes (blue arrowheads). The red horizontal line in the fundus images represents the cross sectional plane of OCT imaging. Scale bars = 100  $\mu\text{m}$ .

**Figure 2.** Increased tumor growth rate in *Kifl4*;TAg-RB mice compared to TAg-RB controls. Representative images of tumor burden in *Kifl4*;TAg-RB mice (*b, d*) compared to TAg-RB mice (*a, c*) at weeks 8 (*a, b*) and 12 (*c, d*) of age by funduscopy (upper panels) and OCT (lower panels). Example tumor masses are marked with yellow arrowheads. Scale bars = 100  $\mu\text{m}$ . (*e*) Discrete visible tumor number in *Kifl4*;TAg-RB eyes vs. TAg-RB control eyes shows a non-significant trend towards a difference ( $p > 0.05$ ; Student's *t*-test;  $n = 4\text{--}6$  per group). (*f*) Growth rates of centrally located retinoblastomas from *Kifl4*;TAg-RB mice (red lines) ( $n = 4$ ) and TAg-RB control mice (black lines) ( $n = 3$ ). Doubling times were significantly different (1.8 vs. 2.9 weeks,  $p < 0.0001$ , extra sum of squares *F*-test).

**Figure 3.** Total tumor burden is increased in *Kifl4*;TAg-RB mice compared to TAg-RB littermate controls. Representative TAg IHC (brown staining) and corresponding H&E images of peripheral tumors at 8 (*a, c, e, g*) and 12 (*b, d, f, h*) weeks comparing TAg-RB mice (*a–d*) with *Kifl4*;TAg-RB littermates (*e–h*). Scale bar = 200  $\mu\text{m}$ . Quantitative IHC analysis (*i*) or H&E analysis (*j*) of percentage tumor burden in *Kifl4*;TAg-RB mice compared to TAg-RB controls. Significant differences were observed at both weeks 8 and 12 by both methods (\*,  $p < 0.05$ ; \*\*,  $p < 0.01$ , Student's *t*-test,  $n = 4\text{--}6$  per group).

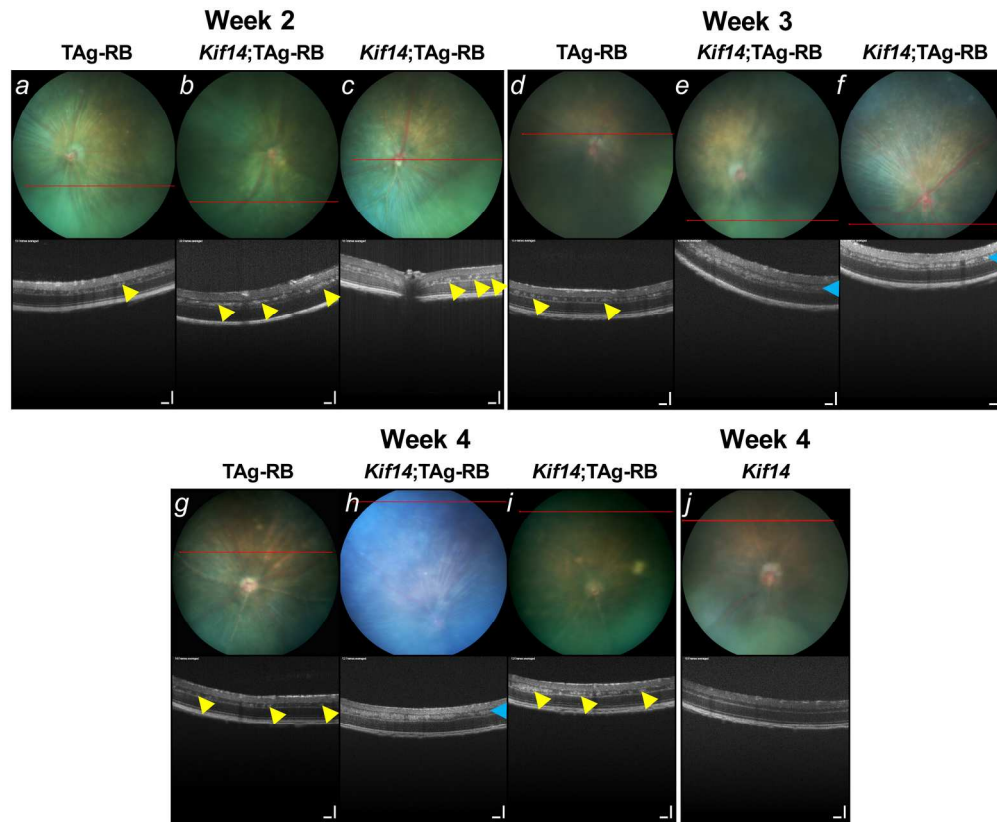


Figure 1. Kif14 overexpression accelerates tumor initiation in TAg-RB. Increased tumor burden in Kif14;TAg-RB mice (b, c, e, f, h, i) vs. TAg-RB controls (a, d, g); the retinas of Kif14 single transgenic mice were normal (j). Representative images at 2–4 weeks of age as visualized by fundus images (upper panels) and OCT (lower panels). Example tumor cell clusters are marked (yellow arrowheads); the entire inner nuclear layer was filled with early tumor cells in some double transgenic eyes (blue arrowheads). The red horizontal line in the fundus images represents the cross sectional plane of OCT imaging. Scale bars = 100  $\mu$ m. 186x152mm (300 x 300 DPI)

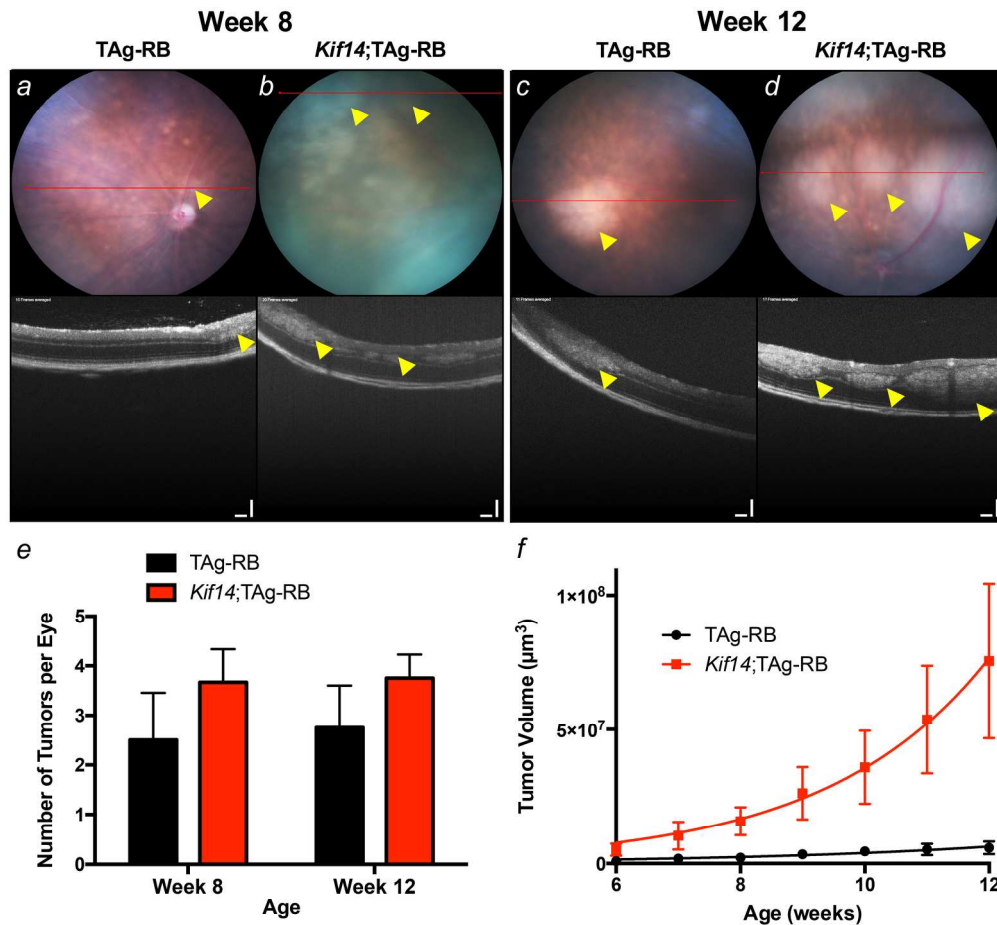


Figure 2. Increased tumor growth rate in *Kif14*;TAg-RB mice compared to TAg-RB controls. Representative images of tumor burden in *Kif14*;TAg-RB mice (b, d) compared to TAg-RB mice (a, c) at weeks 8 (a, b) and 12 (c, d) of age by funduscopy (upper panels) and OCT (lower panels). Example tumor masses are marked with yellow arrowheads. Scale bars = 100  $\mu\text{m}$ . (e) Discrete visible tumor number in *Kif14*;TAg-RB eyes vs. TAg-RB control eyes shows a non-significant trend towards a difference ( $p > 0.05$ ; Student's t-test;  $n = 4-6$  per group). (f) Growth rates of centrally located retinoblastomas from *Kif14*;TAg-RB mice (red lines) ( $n = 4$ ) and TAg-RB control mice (black lines) ( $n = 3$ ). Doubling times were significantly different (1.8 vs. 2.9 weeks,  $p < 0.0001$ , extra sum of squares F-test).  
199x183mm (300 x 300 DPI)

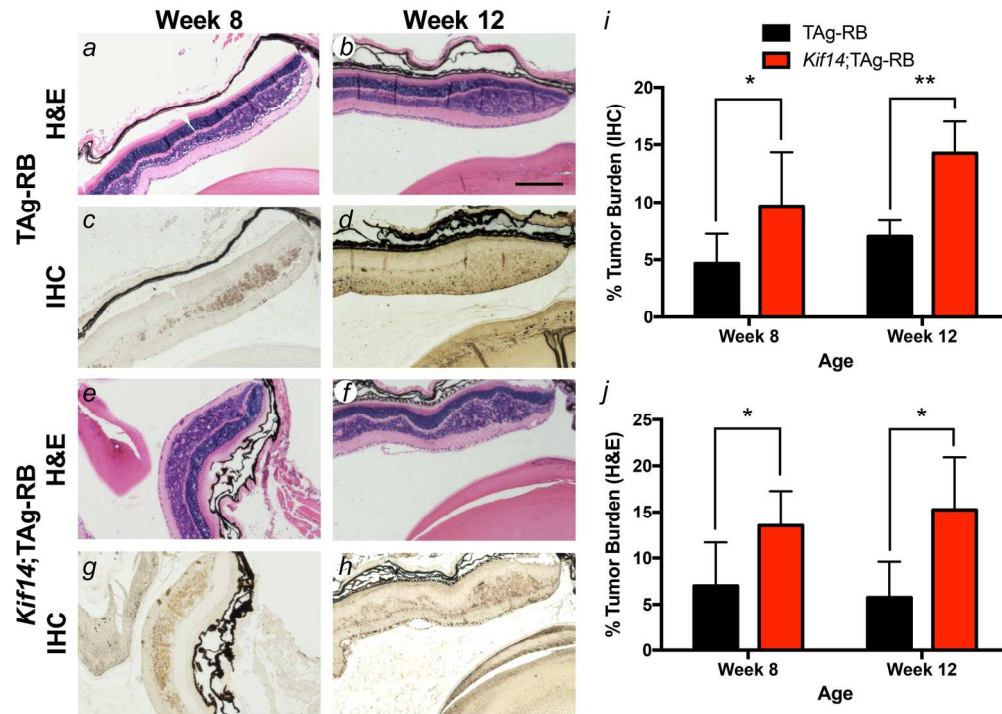


Figure 3. Total tumor burden is increased in Kif14;TAG-RB mice compared to TAG-RB littermate controls. Representative TAG IHC (brown staining) and corresponding H&E images of peripheral tumors at 8 (a, c, e, g) and 12 (b, d, f, h) weeks comparing TAG-RB mice (a–d) with Kif14;TAG-RB littermates (e–h). Scale bar = 200  $\mu$ m. Quantitative IHC analysis (i) or H&E analysis (j) of percentage tumor burden in Kif14;TAG-RB mice compared to TAG-RB controls. Significant differences were observed at both weeks 8 and 12 by both methods (\*,  $p < 0.05$ ; \*\*,  $p < 0.01$ , Student's t-test,  $n = 4$ –6 per group).

167x119mm (300 x 300 DPI)